Real time imaging of femtosecond laser induced nano-neurosurgery dynamics in *C. elegans*

Susana I. C. O. Santos,[1] Manoj Mathew,[1] and Pablo Loza-Alvarez[1,*]

[1]*ICFO-Institut de Ciències Fotòniques, Mediterranean Technology Park, 08860, Castelldefels (Barcelona), Spain*
** pablo.loza@icfo.es*

Abstract: In this study we present for the first time the use of confocal microscopy and laser scanning brightfield microscopy (LSBF) for real time imaging of femtosecond laser nanosurgery and its dynamics in *C. elegans*. A single multimodal optical workstation that provides the ability to perform femtosecond laser nanosurgery and simultaneous confocal and LSBF imaging was used for the purpose. With this tool several dynamic phenomena concomitant with laser nanosurgery in *C. elegans* were observed and imaged. Some of these dynamic phenomena, like muscular contraction and single muscle cell stimulation, have been imaged for the first time during nano-neurosurgery of *C. elegans*.

OCIS codes: (180.0180) Microscopy; (170.1020) Ablation of tissue; (170.3880) Medical and biological imaging

References and links

1. N. Shen, D. Datta, C. B. Schaffer, P. LeDuc, D. E. Ingber, and E. Mazur, "Ablation of cytoskeletal filaments and mitochondria in live cells using a femtosecond laser nanoscissor," Mech. Chem. Biosyst. **2**(1), 17–25 (2005).
2. H. Hirase, V. Nikolenko, J. H. Goldberg, and R. Yuste, "Multiphoton Stimulation of Neurons Multiphoton stimulation of neurons," Neurobiol. **51**(3), 237–247 (2002).
3. R. L. Amy, and R. Storb, "Selective mitochondrial damage by a ruby laser microbeam: an electron microscopic study," Science **150**(3697), 756–758 (1965).
4. M. F. Yanik, H. Cinar, H. N. Cinar, A. D. Chisholm, Y. Jin, and A. Ben-Yakar, "Neurosurgery: functional regeneration after laser axotomy," Nature **432**(7019), 822 (2004).
5. R. R. Gattass, L. R. Cerami, and E. Mazur, "Micromachining of bulk glass with bursts of femtosecond laser pulses at variable repetition rates," Opt. Express **14**(12), 5279–5284 (2006), http://www.opticsinfobase.org/oe/abstract.cfm?URI=oe-14-12-5279.
6. S. M. Eaton, H. B. Zhang, P. R. Herman, F. Yoshino, L. Shah, J. Bovatsek, and A. Arai, "Heat accumulation effects in femtosecond laser-written waveguides with variable repetition rate," Opt. Express **13**(12), 4708–4716 (2005), http://www.opticsinfobase.org/oe/abstract.cfm?URI=oe-13-12-4708.
7. Z. Wu, A. Ghosh-Roy, M. F. Yanik, J. Z. Zhang, Y. Jin, and A. D. Chisholm, "Caenorhabditis elegans neuronal regeneration is influenced by life stage, ephrin signaling, and synaptic branching," Proc. Natl. Acad. Sci. U.S.A. **104**(38), 15132–15137 (2007).
8. S. Psilodimitrakopoulos, S. I. C. O. Santos, I. Amat-Roldan, A. K. N. Thayil, D. Artigas, and P. Loza-Alvarez, "In vivo, pixel-resolution mapping of thick filaments' orientation in nonfibrilar muscle using polarization-sensitive second harmonic generation microscopy," J. Biomed. Opt. **14**(1), 014001 (2009).
9. P. J. Campagnola, and L. M. Loew, "Second-harmonic imaging microscopy for visualizing biomolecular arrays in cells, tissues and organisms," Nat. Biotechnol. **21**(11), 1356–1360 (2003).
10. W. Denk, J. H. Strickler, and W. W. Webb, "Two-photon laser scanning fluorescence microscopy," Science **248**(4951), 73–76 (1990).
11. J. Squier, M. Muller, G. Brakenhoff, and K. R. Wilson, "Third harmonic generation microscopy," Opt. Express **3**(9), 315–324 (1998), http://www.opticsinfobase.org/oe/abstract.cfm?URI=oe-3-9-315.
12. D. Yelin, and Y. Silberberg, "Laser scanning third-harmonic-generation microscopy in biology," Opt. Express **5**(8), 169–175 (1999), http://www.opticsinfobase.org/oe/abstract.cfm?URI=oe-5-8-169.
13. E. J. Gualda, G. Filippidis, G. Voglis, M. Mari, C. Fotakis, and N. Tavernarakis, "In vivo imaging of cellular structures in Caenorhabditis elegans by combined TPEF, SHG and THG microscopy," J. Microsc. **229**(1), 141–150 (2008).
14. E. J. Gualda, G. Filippidis, M. Mari, G. Voglis, M. Vlachos, C. Fotakis, and N. Tavernarakis, "*In vivo* imaging of neurodegeneration in *Caenorhabditis elegans* by third harmonic generation microscopy," J. Microsc. **232**(2), 270–275 (2008).

#119494 - $15.00 USD Received 3 Nov 2009; revised 18 Dec 2009; accepted 18 Dec 2009; published 24 Dec 2009

15. S. H. Chung, and E. Mazur, "Femtosecond laser ablation of neurons in *C. elegans* for behavioral studies," Appl. Phys., A Mater. Sci. Process. **96**(2), 335–341 (2009).
16. M. F. Yanik, H. Cinar, H. N. Cinar, A. Chisholm, Y. Jin, and A. Ben-Yakar, "Nerve regeneration in Caenorhabditis elegans after femtosecond laser axotomy," IEEE J. Quantum Electron. **12**, 1283–1291 (2006).
17. F. Zeng, C. B. Rohde, and M. F. Yanik, "Sub-cellular precision on-chip small-animal immobilization, multi-photon imaging and femtosecond-laser manipulation," Lab Chip **8**(5), 653–656 (2008).
18. M. Mathew, S. I. C. O. Santos, D. Zalvidea, and P. Loza-Alvarez, "Multimodal optical workstation for simultaneous linear, nonlinear microscopy and nanomanipulation: upgrading a commercial confocal inverted microscope," Rev. Sci. Instrum. **80**(7), 073701 (2009).
19. http://www.nikoninstruments.com/Products/Microscope-Systems/Inverted- Microscopes/Biological/Eclipse-Ti.
20. S. Brenner, "The genetics of *Caenorhabditis elegans*," Genetics **77**(1), 71–94 (1974).
21. F. Bourgeois, and A. Ben-Yakar, "Femtosecond laser nanoaxotomy properties and their effect on axonal recovery in C. elegans," Opt. Express **16**(8), 5963–15963 (2008), http://www.opticsinfobase.org/oe/abstract.cfm?URI=oe-16-8-5963.
22. A. Vogel, J. Noack, G. Hüttmann, and G. Paltauf, "Mechanisms of femtosecond laser nanosurgery of cells and tissues," Appl. Phys. B **81**(8), 1015–1047 (2005).
23. N. I. Smith, Y. Kumamoto, S. Iwanaga, J. Ando, K. Fujita, and S. Kawata, "A femtosecond laser pacemaker for heart muscle cells," Opt. Express **16**(12), 8604–8616 (2008), http://www.opticsinfobase.org/oe/abstract.cfm?URI=oe-16-12-8604.
24. M. C. Hogan, C. M. Stary, R. S. Balaban, and C. A. Combs, "NAD(P)H fluorescence imaging of mitochondrial metabolism in contracting Xenopus skeletal muscle fibers: effect of oxygen availability," Appl. Physiol **98**(4), 1420–1426 (2005).

1. Introduction

Light and lasers are increasingly being used as manipulation tools for biological samples and there are several applications that can range from organelle nanosurgery [1], to cell growth stimulation [2]. The use of laser as a scalpel started few decades ago when Amy and Storb (1965) used a laser beam to "selectively damage" mitochondria [3]. Ever since, there have been significant developments in the technique and recently neuronal processes of few hundred nanometer thickness have been precisely incised without any apparent collateral damage [4].

Among the various laser systems in use for this purpose the ultrashort pulsed (femotsecond\picosecond) lasers stand out due to the many advantages they possess. The most significant being the confinement of induced effects primarily to the focal volume (<1 femtolitre) of the tightly focused laser beam, owing to the involvement of nonlinear absorption mechanisms in the ablation process. The use of femtosecond laser sources of different wavelengths and pulse repetition rate regimes (MHz and KHz) has been widely considered and different sources are used for different targets and samples [5,6]. Moreover, femtosecond lasers with low repetition rates (KHz) and high repetition rates (MHz) have been successfully employed to precisely incise, individual neuronal processes [7].

Live *Caenorhabditis elegans* (*C. elegans*) can be imaged using a wide range of optical techniques. The most commonly used are Differential Interference Contrast (DIC), Phase Contrast (PC), Epi-fluorescence (EF) and Multichannel Confocal (MCC) microscopy. Modern commercial confocal microscopes combine most of the above-mentioned imaging techniques and, in recent times, even spectrally resolved confocal microscopy. All these together, in addition to fully automated components, software control and image processing/analysis tools, make commercial confocal microscopes extremely versatile and user-friendly devices to be the elected tool by most biologists.

Nonlinear imaging is starting to emerge as a novel tool in the study of this nematode, especially in the study of muscle with Second Harmonic Generation (SHG) [8,9]. Advances in nonlinear/multiphoton microscopy, overcomes some drawbacks inherent in linear imaging techniques such as low penetration depths and "out of focal plane" sample photodamage/photobleaching (highly relevant for long time-lapse experiments). This is mainly due to the use of ultrashort Near Infrared (NIR) optical pulses for excitation, instead of the commonly used Ultraviolet (UV) wavelengths used in linear fluorescence techniques. Second and Third Harmonic Generation (SHG and THG, respectively) microscopy goes a step

#119494 - $15.00 USD Received 3 Nov 2009; revised 18 Dec 2009; accepted 18 Dec 2009; published 24 Dec 2009

further by providing intrinsic contrast (without need for any labelling) [8–14] and structural information below the resolution limit of light [8,9]. Furthermore, the nonlinear microscope using the femtosecond laser can easily be used to perform nano-manipulation techniques such as nanosurgery [4]. So far, real time imaging of laser axotomy in *C. elegans* has only been done with Epi-fluorescence and DIC microscopy [4,15,16] and, more recently with two-photon imaging [17].

The nonlinear\multiphoton microscope, when used to perform nanosurgery, can also be used to obtain high axial-resolution multiphoton images of the targeted area before and after the process of nanosurgery is performed. This way of imaging before and after, however, has the drawback that many dynamic phenomena that occur during the nanosurgery procedure can be missed out due to the lack of simultaneous imaging capability. A tool that provides a combination of different imaging modalities that allows imaging the process of nanosurgery and the various phenomena taking place along with it in real time is yet missing.

In this study we present, for the first time to our knowledge, the possibility to simultaneously image highly dynamic phenomena occurring during the femtosecond laser nanosurgery of neuronal axons in *C. elegans* with a high axial resolution technique such as with confocal microscopy. Moreover, we present the possibility of using a multimodal workstation [18] that allows *simultaneous* imaging of the surgical process, by both linear and multiphoton\nonlinear imaging techniques during laser nanosurgery. High resolution (both axial and radial) imaging when performed during the surgical process is essential for a correct assessment of the efficiency of the procedure and is critical for the accurate study of the procedure as a physical phenomenon and to study the dynamic phenomena that occur during the procedure of nanosurgery. The use of this multimodal workstation allowed us to image, for the first time, several of the here reported active phenomena related with the laser axotomy. The fine details of these phenomenon can be used for improving the above-mentioned laser manipulation tool and provide valuable information about the optical surgical process itself.

2. Materials and methods

2.1. The multimodal workstation

A nonlinear/multiphoton microscope is built around a commercial confocal (Nikon C1-Si) inverted microscope (Nikon Eclipse Ti-E14, Nikon Inc., Japan [19]) in a way that both the confocal and multiphoton sections can work independently and simultaneously (see Fig. 1). All the flexibility offered by the commercial confocal system (such as: two filter turrets, four detection ports, DIC condenser and diascopic detector) was fully exploited for the development of this workstation. Moreover, a separate scanning system, separate detection systems, both in the forward and backward directions and separate control systems and software were added for the multiphoton section.

#119494 - $15.00 USD Received 3 Nov 2009; revised 18 Dec 2009; accepted 18 Dec 2009; published 24 Dec 2009

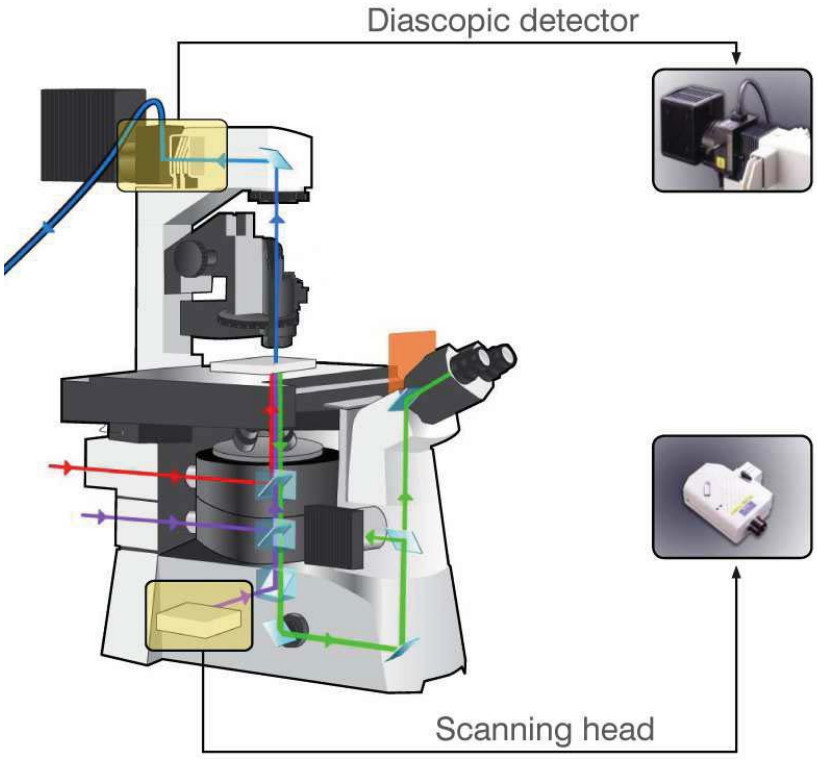

Fig. 1. Schematic of the multimodal workstation with its various light paths. Green light path-backward detected fluorescence, violet light path-epi-fluorescence and confocal excitation, blue light path-forward propagating signal from laser scanning confocal brightfield, red light path-NIR excitation used for laser surgery. The diascopic detector forwards the signal from $LSBF_C$ into an optical fibre. Note the use of two filter turrets [see ref. (18) for details].

The main advantage of this workstation is its ability to perform real time multi channel confocal microscopy or epi-fluorescence (EF) microscopy while performing femtosecond laser induced manipulation. This multimodal workstation has as main capabilities: simultaneous Laser Scanning Brightfield ($LSBF_M$), SHG and TPEF imaging; simultaneous Confocal, $LSBF_M$ and SHG imaging, simultaneous EF, $LSBF_M$ and SHG imaging, simultaneous Confocal imaging, $LSBF_C$ imaging and Femtosecond laser induced stimulation/manipulation, simultaneous EF imaging and Femtosecond laser induced stimulation/manipulation [18]. Please note that the workstation has ability to detect the forward scattered excitation light and simultaneously generate a topography image or a bright field image along with other modalities (imaging\manipulation). This is referred to here as LSBF. Since this is done by detecting the forward scattered ultrashort NIR light in the multiphoton mode and detecting the UV excitation light in the confocal mode using separate apparatus, for the sake of clarity they are respectively referred to as $LSBF_M$ and $LSBF_C$.

2.2. Worm mounting

C. elegans strains were maintained using standard procedures [20]. A number of healthy worms were mounted on a thin 2% agar pad with an anaesthetic between two 40μm glass slides. The selected anaesthetic for immobilisation was sodium azide - NaN3 (0,8μl at 25mM). The worm mounts were only used within a period of less than half an hour in order to guarantee the worm physical condition. Used strain was the transgenic strain juIs76 [unc-25::gfp] II which has GFP labelled D-type motoneurons. The choice of this specific set of

#119494 - $15.00 USD Received 3 Nov 2009; revised 18 Dec 2009; accepted 18 Dec 2009; published 24 Dec 2009

neurons was made for two main reasons. The size of the axonal commissures (approximately 300nm diameter) and their location (isolated and extremely close - approximately 200nm, to body wall muscles and to the worm's cuticle).

2.3. Nano-neurosurgery and simultaneous imaging

A nonlinear microscope can readily be converted into a nanosurgery station by directing the femtosecond laser beam at very high intensity (above the damage threshold) to a selected target using the same laser scanning system as used for imaging. The workstation here described provides the possibility for two independent laser scanning systems and one of its strengths is its ability to perform simultaneous imaging with the confocal section while, at the same time, the multiphoton part performs the nanosurgery.

Incisions were made on the commissures of the worm's D-type motoneurons on the first third of the axon portion, in close proximity to either the ventral or the dorsal cord. To select a target the multiphoton section of the multimodal workstation is first operated in the imaging mode to obtain a TPEF image of the targeted neuron. A target is selected using a graphic user interface (GUI) based on this TPEF image. Since the laser beam used for TPEF imaging is the same to be used subsequently in surgery, this way of target selection enables precise determination of the focal plane for a more efficient incision. The multiphoton section of the multimodal workstation is subsequently switched to surgery mode. The laser beam is focused on to the target through the same high numerical aperture oil immersion objective lens (CFI Plan Apochromat 60x, NA = 1.4), as used for imaging. Axotomy is performed by increasing the average power upto 90mW (~1.2nj/pulse, 868nm at 76MHz repetition rate) on the sample plane, by keeping the femtosecond beam static on the selected axonal target for 200ms (interaction time controlled by the use of a home-made electronic shutter).

Simultaneous imaging of the process of nano-neurosurgery could be preformed with the following techniques: (1) Brightfield (BF) and (2) Epi-Fluorescence (EF) imaging, both using a CCD camera; (3) Three Channel Confocal (3CC) imaging and (4) Laser Scanning Brightfield (LSBF) Imaging. The three channels in the confocal microscope refers to the blue (515/30nm), green (590/50nm) and red (650nmLP) detection channels provided in the confocal microscope. The three detection channels together with the $LSBF_C$ image provides, four images from four different channels (blue, green, red and brightfield) which were obtained simultaneously, either separately or combined.

3. Results

3.1. Simultaneous laser axotomy and high resolution imaging

Laser axotomy was preformed in D-type axonal neurons of *C. elegans* using MHz femtosecond laser. More than 90 laser incisions on neuronal axons were performed by placing a static NIR femtosecond laser beam (868nm with an average power of about 90mW (~1.2 nj/ pulse) at 76 MHz repetition rate) on the targeted area for an exposure time of 200ms. All the incisions were visualized simultaneously with 3CC (green, blue and red channels) microscopy (using 488nm and 457nm as the excitation source) and $LSBF_C$ imaging.

During the study of laser axotomy a number of dynamic events were observed live mainly using 3CC and $LSBF_C$ imaging. These were: (1) GFP spilling from severed axon tips; formation of cavitation bubbles that would either (2) open a hole through the cuticle or (3) displace the neuronal axon; (5) muscular reaction and contraction in response to laser impact; (5) spreading of autofluorescence in one single muscular cell and (6) damage of the surrounding areas with increased autofluorescence. These active processes can take from few milliseconds (such as the GFP spilling that occurs promptly) to few tens of seconds. In Table 1, a summary of the above mentioned observed dynamic event, the technique used to image the phenomena, an approximate duration of the event and reference to illustrations of the event can be found.

#119494 - $15.00 USD Received 3 Nov 2009; revised 18 Dec 2009; accepted 18 Dec 2009; published 24 Dec 2009

Table 1. Observed dynamic effects, their duration and the imaging techniques used to visualise each effect. 3CC – three channel confocal microscopy; $LSBF_C$ –confocal laser scanning brightfield

Observed dynamic effect (n)	Imaging Technique	Duration of the effect	Illustrations
GFP spilling (16)	3CC	Immediate up to 30s	Figure 2
Cuticle elasticity (12)	$LSBF_C$	Immediate up to 15s	Figure 3
Neuronal displacement and elasticity (6)	3CC	Immediate up to 15s	Figure 4
Muscular contraction (29)	$LSBF_C$, 3CC	Immediate up to 5s	Figure 5
Spreading of autofluorescence in a single muscle cell (12)	3CC	Immediate up to few seconds	Figure 6
Increased autofluorescence (60)	3CC	Long	Figure 7

One of the effects that is quite often observed during the nanosurgery procedure and that extends to a considerate amount of time is the appearance of autofluorescence in the regions surrounding the point of impact of the laser spot. This effect depends on the amount of collateral damage to the regions surrounding the laser surgery. This can be used as a reasonable indicator of the induction of collateral damage to surrounding structures as a result of laser impacting the axon (see Fig. 7).

During the process of nano-neurosurgery another effect that can be observed by 3CC microscopy is the bursting and spilling of GFP enriched axoplasm of either one or both severed axon tips. All neurosurgeries here reported were performed on neurons expressing GFP in their axoplasm. When the axon is severed, thanks to the ability of simultaneous imaging it is possible to observe that the axoplasm spills out in the form of green droplets. Figure 2(a) shows the selected region before the surgical procedure and Fig. 2 (b-l) show the dynamics of the process throughout time. The droplets of GFP in most cases continue to flow out for approximately 15 seconds. This kind of dynamic process had been reported previously by F. Bourgeois and A. Ben-Yakar [21].

#119494 - $15.00 USD Received 3 Nov 2009; revised 18 Dec 2009; accepted 18 Dec 2009; published 24 Dec 2009

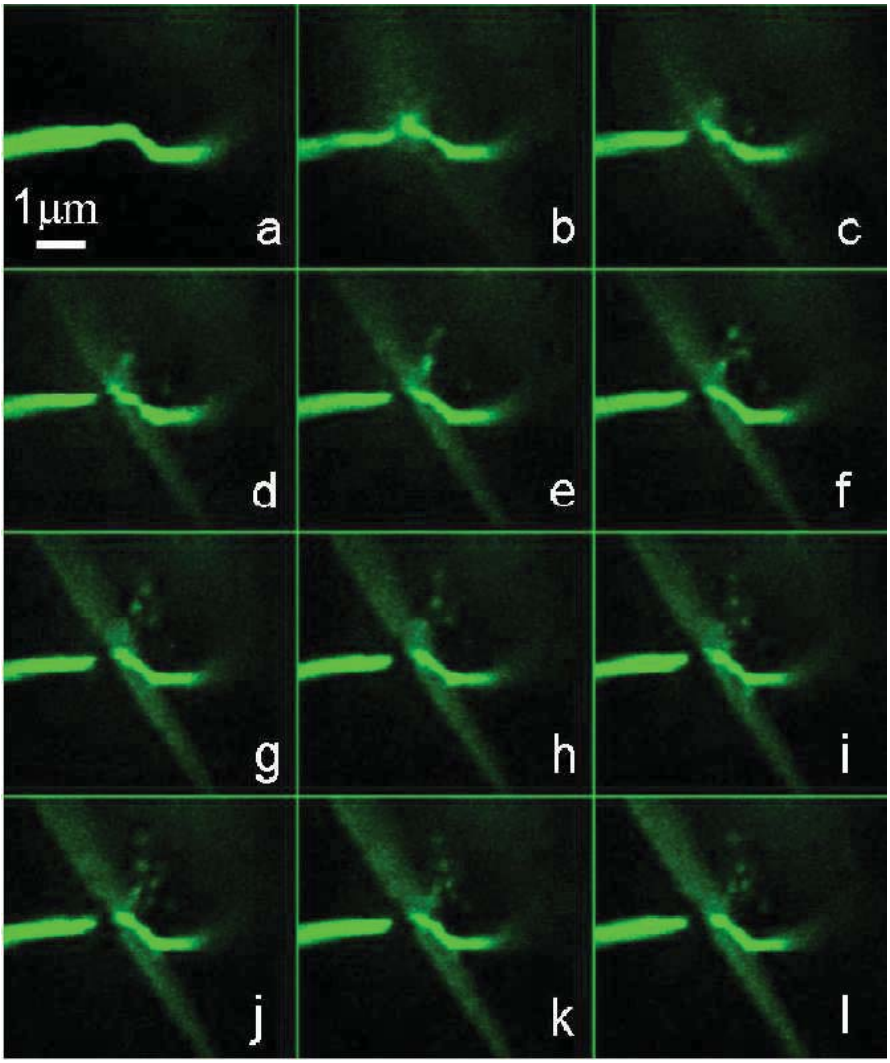

Fig. 2. Time-lapse images depicting GFP expressing axoplasm spilling and bursting from D-type motoneurons in *C. elegans*. (a) Before incision; (b-l) evolution of axoplasm spilling after nanosurgery. Time between frames: 1 second. Imaging of this dynamic process was done with confocal microscopy using 488nm for excitation.

One other dynamic effect that could be observed during the nano-neurosurgery procedure is the formation of cavitation bubbles that can either open a hole through the cuticle (Fig. 3) or displace the neuronal axon (Fig. 4). In case of femtosecond laser induced nanosurgery the point of energy deposition is well confined to the focal volume of the impacting laser beam. However, the cavitation bubble formed as a result of this process happening in a liquid media (a biological sample) can, sometimes, propagate and create interesting effects in the surroundings. An example of such an effect is the aperture/closure of the worm's cuticle. The formation of the bubble opens up a hole (usually 2-3µm wide) in the cuticle immediately after the laser impact. The cuticle opening, however, closes back in a matter of few seconds. This is evidence of the elasticity of the collagen structure of the cuticle and can be an interesting phenomenon. Figure 3 shows the $LSBF_C$ image of the worm's midbody region before (a) and after (b) the application of the femtosecond laser beam for nanosurgery. Figure 3(b) shows the opening of the cuticle soon after the laser beam impacts on the neuron commissure. The

#119494 - $15.00 USD Received 3 Nov 2009; revised 18 Dec 2009; accepted 18 Dec 2009; published 24 Dec 2009

opened hole closed back in about 6 seconds (Fig. 3 (c-i)). The time duration of this process in general can vary between few seconds up to 15 seconds depending on the operated case.

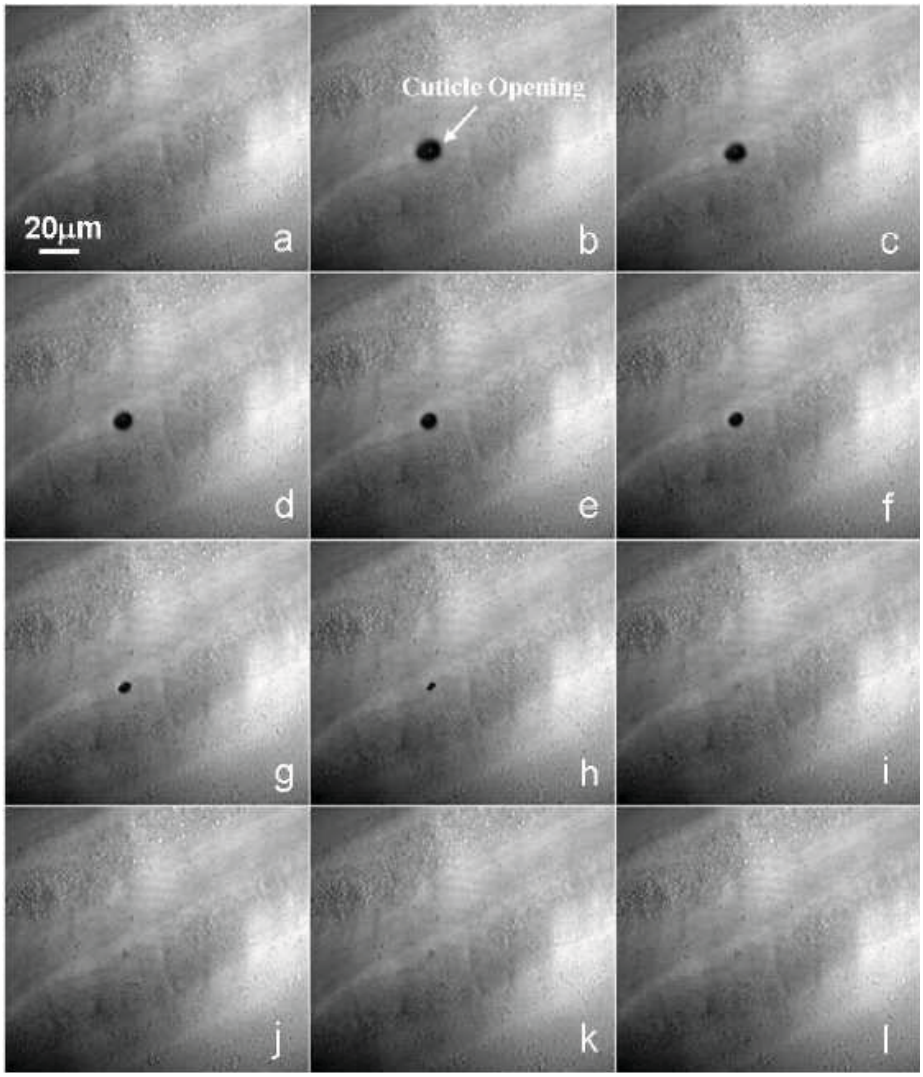

Fig. 3. Confocal laser scanning brightfield ($LSBF_C$) images of the dynamics of cuticle opening and closure as result of induced bubble during a process of laser nanosurgery. a- before surgical intervention; b-l dynamics of cuticle opening/closure. Time between frames: 1 second.

In few cases during the impact of the laser on the targeted structure the cuticle opening resulting due to the cavitation bubble displaces the neuronal axon without severing it. Subsequently as the cuticle opening closes back, the axon relaxes back to its original anatomical location. This phenomenon occurs when a slight inaccuracy was committed in the selection of the target. The stretching and relaxation of the neuronal axon was found to be caused by the opening up of the hole in the cuticle, and its subsequent closure. The opened hole stretches and displaces the axon, which relaxes back as the hole closes. One such case is depicted in Fig. 4. Figure 4(a) shows the confocal fluorescence image of the targeted region before the surgical procedure and Fig. 4 (b-o) show the dynamic process that can be visualised with a single green channel (left hand figure) or with the aid of a superposition of the blue and the green channels (right hand figure). The blue autofluorescence that was observed in the

#119494 - $15.00 USD Received 3 Nov 2009; revised 18 Dec 2009; accepted 18 Dec 2009; published 24 Dec 2009

right hand figures is obtained with simultaneous excitation of the sample with 457nm (in addition to the 488nm excitation used for the GFP excitation). The blue autofluorescence appears in the region where the bubble opens a hole in the cuticle. Apparently the autofluorescence is produced as result of the stretching of the collagenous cuticle since the autofluorescence disappears as the cuticle closes back.

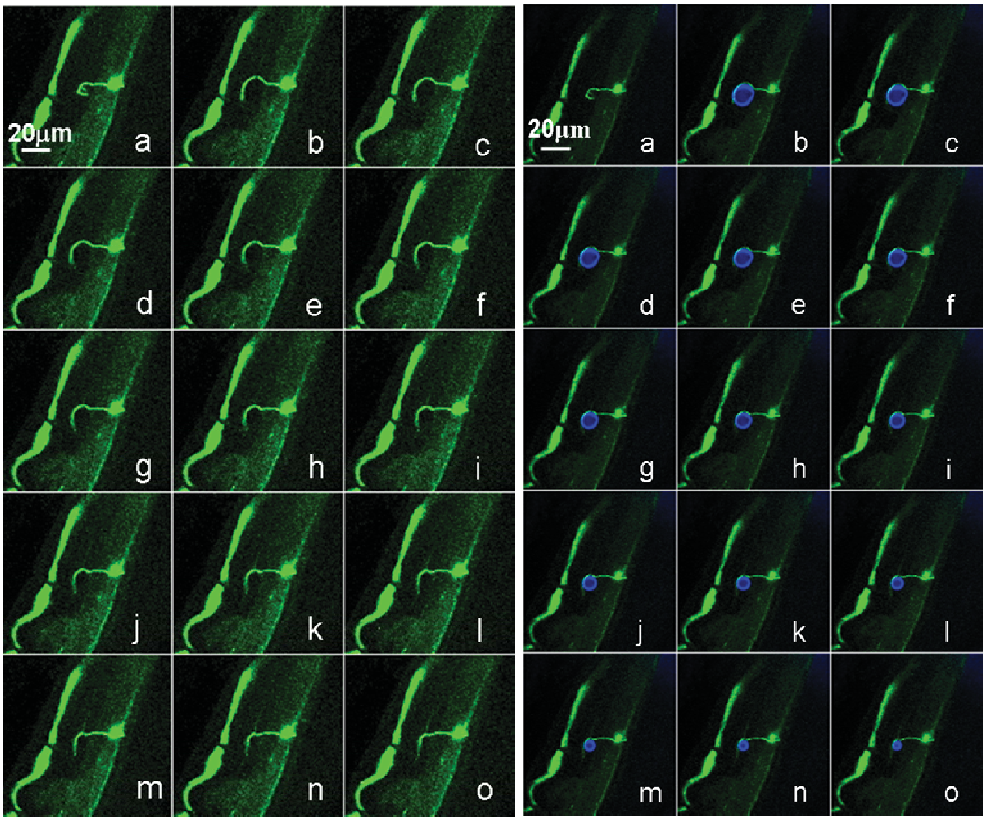

Fig. 4. Time lapse confocal images of both the green (left hand figure) and the superposed blue and green (right hand figure) channels of axonal displacement by the cuticle hole and the resultant blue autofluorescence as a result of the cavitation bubble. a-before surgical procedure; b-o evolution of the process. Time between frames: 1 second.

In some cases the anaesthetised worm reacts to the impact of the laser during nanosurgery and muscular contraction in the immediate vicinity of the laser impact spot is observed. The muscle contracts immediately after laser impact and takes few seconds to relax back. This effect can be observed in Fig. 4 where confocal laser scanning brightfield ($LSBF_C$) images are depicted. To facilitate observation of the effect, the position of a prominent anatomical reference in the image was marked using horizontal and vertical guidance dashed lines. Muscular contraction results in the movement of the whole midbody region and lasts approximately 4 seconds. After the contraction the muscles relax back. This effect is better appreciated in the media file depicted in Fig. 6.

#119494 - $15.00 USD Received 3 Nov 2009; revised 18 Dec 2009; accepted 18 Dec 2009; published 24 Dec 2009

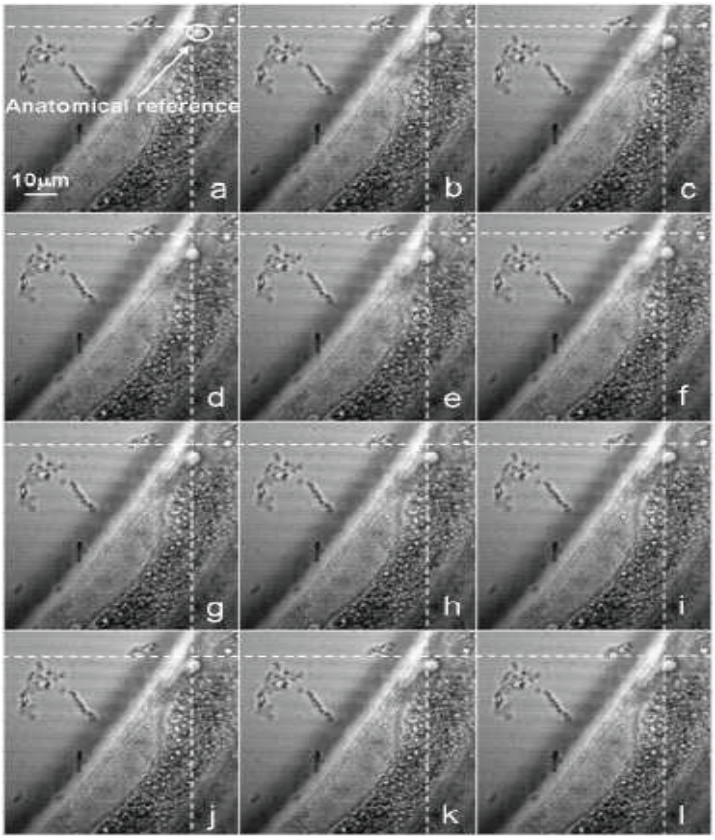

Fig. 5. Time lapse confocal laser scanning brightfield images showing worm's muscular contraction as a result of the impact of the laser beam used for laser nanosurgery. a- before surgical procedure; b-l- time evolution of muscular contraction. Horizontal and vertical dashed lines are marking a prominent anatomical reference to aid in the observation of this active process. Time between frames: 1 second.

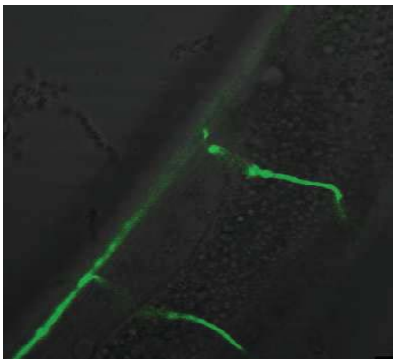

Fig. 6. Time lapse movie of laser induced muscular contraction. The movie shows the superposition of the green channel (showing the axons of neurons) as well as the $LSBF_C$ channel (showing the midbody of the worm). Laser impact incises the axon and at the same time induces muscular contraction which is seen as the movement of the whole midbody (Media 1).

One other significant effect that is observed in many of our operated worms during laser nanosurgery is the spreading of green autofluorescence through a single muscle cell as the laser scalpel impacts a point on an axon that passes above that muscle cell. This is much

#119494 - $15.00 USD Received 3 Nov 2009; revised 18 Dec 2009; accepted 18 Dec 2009; published 24 Dec 2009

unlike the observed autofluorescence mentioned above resulting from collateral tissue damage. In this case the autofluorescence spreads as a wave from the impact point throughout the whole cell. This process takes few seconds (results not shown). Interestingly the increased autofluorescence is limited to that particular muscle cell that lies just below the point of laser impact and does not spread to adjacent muscle cells. In addition the autofluorescence does not spread into the nucleus. Figure 7 shows the dynamics of the green autofluorescence spreading through a single muscle cell starting at the point of impact of the laser in the operated worm and identifying clearly the cell boundaries. The nucleus can be seen as a dark circle devoid of increased autofluorescence

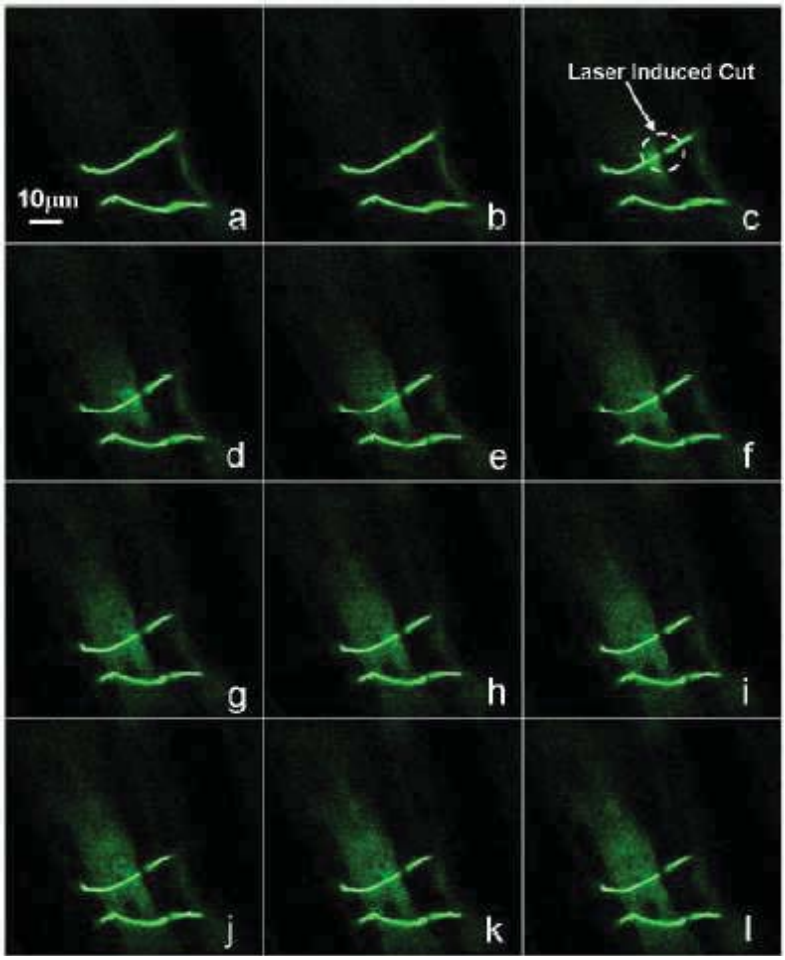

Fig. 7. Time lapse images showing the spreading of autofluorescence in a single body wall muscle cell. a- before surgical procedure; b- evolution of the phenomenon during nanosurgery. Images obtained with confocal fluorescence microscopy using 488nm as excitation source. Time between frames: 1 second.

Figure 8 shows a case that brings out the difference between autofluorescence increase due to collateral damage and autofluorescence spreading in a single muscle cell as a result of muscular stimulation. Axon-1 was incised before axon-2 (Fig. 8(a)) and it resulted in spreading of green autofluorescence in the muscle cell just below it. The cell boundary is clearly visible. Incision on axon-2 resulted in collateral damage and increased autofluorescence around the point of incision in the form of a circle of diameter around 1μm (Fig. 8(b)).

#119494 - $15.00 USD Received 3 Nov 2009; revised 18 Dec 2009; accepted 18 Dec 2009; published 24 Dec 2009

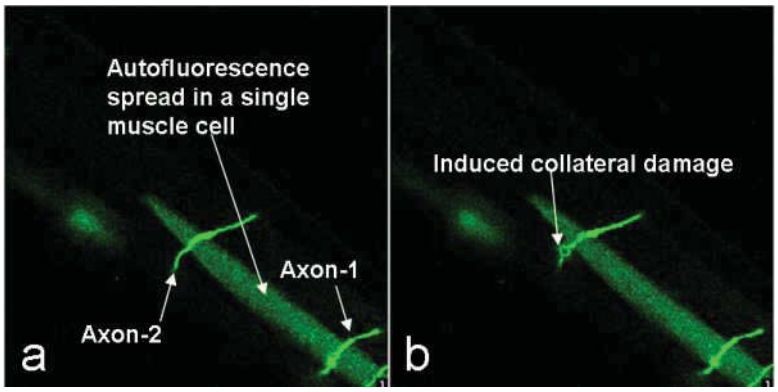

Fig. 8. Difference between increased autofluorescence due to collateral damage and single muscle cell stimulation. a- before surgical procedure on axon-2; b- after surgical procedure on axon-2. Nanosurgery on axon-1 was performed before being performed on axon-2.

4. Discussion

More than 90 laser incisions of neuronal axons were made by placing a static femtosecond beam on the targeted area for an exposure time of 200ms (See Table 1). All the incisions were visualized in real time. During simultaneous imaging of the nano-neurosurgery procedure a number of dynamic phenomena were observed such as: damage of the surrounding areas with increased autofluorescence, GFP bursting and spilling from severed axon tips, formation of cavitation bubbles that would either open a hole through the cuticle or displace the neuronal axon, worm muscular reaction to laser impact and muscular contraction and spreading of autofluorescence in one single muscular cell. These active processes can take from few milliseconds (such as the GFP spilling that occurs promptly) to few tens of seconds. Some of these active processes can be predicted by the thorough study of the mechanisms of femtosecond laser nanosurgery [22].

This work attempts the study of the dynamics of laser axotomy in *C. elegans* by the use of unamplified femtosecond lasers in the MHz repetition rate regime. A group of imaging techniques were used for this purpose in association with femtosecond laser nano-surgery tool and is here presented. This multimodal workstation allowed, within others, the nano-manipulation of the axons in *C. elegans* and real time imaging with different techniques. With the use of the presented multimodal workstation, and more specifically with a femtosecond laser nanosurgery scalpel simultaneously used with single photon imaging, many dynamic phenomena that occur during laser nanosurgery were revealed, to our knowledge, for the first time. Some of these dynamic phenomena, and their impact in the collateral damage assessment of the resulting operated worm, would have been missed out of observation if simultaneous imaging was not used.

Femtosecond laser induced cavitation bubbles and their effect in the sample has been thoroughly predicted and assessed by Vogel [22]. The occurrence of the cavitation bubbles may result in inherent damage that can be due to dissociation of biomolecules into volatile non-condensable fragments. The cavitation bubble opens up a hole in the cuticle in many operated cases, which closes back in a few seconds. The observation of this phenomenon discloses some of the worm's anatomical characteristics that might be of interest to investigate such as the elasticity of the neuronal processes, cuticle and muscular cells. In most of these cases there is apparently no damage in the post surgery observation to any structure including the cuticle where the hole opened. A rigorous assessment of collateral damage, however, requires post surgical observation of the surrounding areas of the incision by the use of other imaging modalities. Imaging tools such as TPEF and SHG microscopy could come in handy for this purpose.

#119494 - $15.00 USD Received 3 Nov 2009; revised 18 Dec 2009; accepted 18 Dec 2009; published 24 Dec 2009

The emergence of increased autofluorescence in the surrounding areas of the laser surgery is also a phenomenon that has been reported before [21]. This usually indicates damage is mainly due to mitochondria destruction at the edge of the laser incision. GFP spilling from the severed axon tips has also been observed before by epi- fluorescence microscopy [21].

A slight interaction between the femtosecond laser spot with the muscles surrounding of axonal areas, while the laser impacts the axon can lead to muscular contraction. Such femtosecond laser induced muscular contraction has been reported in cardiomyocytes [23]. It has been demonstrated that by periodic exposure to femtosecond laser pulse-trains, periodic contraction cycles in cardiomyocytes could be triggered, depleted, and synchronized with the laser periodicity. Muscle contraction is a calcium-signalling dependent process. The calcium ions bind and interact with molecules associated with the cells contractile machinery, the end result being a mechanical contraction. Any means that can induce elevations in calcium ions can as a result induce muscular contraction. Femtosecond laser irradiation is one of these means and can possibly induce muscular contraction and our results are in agreement with this. This is obviously an interesting subject for further research wok.

One other highly appealing subject of future work is the observed spreading of autofluorescence in a single muscular cell after laser impact in the vicinity of the muscle cell. There seems to be laser stimulation of a single cell where a wave of autofluorescence spreads in few seconds through the cell with exception to the cell nucleus. Such increase of intrinsic fluorescence could be explained as a result muscle stimulation and resulting NAD(P)H increasing autofluorescence. There are many factors that can fuel cell NAD(P)H levels such as workload, dehydrogenase activity, and cytosolic-mitochondria compartmentation and, therefore, the interpretation of NAD(P)H fluorescence in intact tissues must be mindful. Nonetheless, single cell muscular stimulation and NAD(P)H increased autofluorescence due to mitochondrial metabolism in contracting cells [24] can be a potentially strong explanation. This subject certainly deserves further study.

Post surgery imaging of the targeted and surrounding regions can also be done using a combination of both linear and nonlinear imaging techniques. The combination of all these high resolution imaging tools could show a great importance/significance not only to the study of the process of laser nanosurgery itself, but also to be able to perfect this technique by assessing the development of the incision and to study the possible inflicted collateral damage. All this can be used to improve the efficiency of this valuable tool of laser nanosurgery. The use of SHG imaging for example of body wall muscles that are close by the axonal processes may also be used as a good indicator of the possible induced collateral damage. In this case the intrinsic signal provided by the intact muscular tissues may be, to some extend, get altered as a result of collateral damage and this imaging technique can aid in the determination of this damage. The multimodal optical workstation setup provides such ability by enabling post-surgical observation of the surgical region using simultaneous SHG and TPEF imaging. This ability would be used in future works for detailed and rigours analysis of collateral damage to muscle. This post-surgical imaging using nonlinear techniques will greatly complement real time imaging in accessing collateral damage. Thus, future efforts will be directed towards experiments in which other linear (with improved temporal resolution capabilities such as spinning discs), and non-linear modalities of imaging (for example based on non-labelling protocols, such as the third harmonic generation technique) could be implemented for better collateral damage assessment.

5. Conclusions

Laser axotomy was preformed on D-type axons of *C. elegans* using MHz femtosecond laser and real time imaging of the procedure was done with confocal fluorescence imaging and laser scanning brightfield imaging. This allowed not only the visualisation of the procedure but also showed potential for the study and to perfect the laser axotomy techniques in biological samples. Moreover, the simultaneous imaging with high axial resolution allowed

#119494 - $15.00 USD Received 3 Nov 2009; revised 18 Dec 2009; accepted 18 Dec 2009; published 24 Dec 2009

the observation and unravelling of dynamic phenomena that happen during the axotomy. This shows a great importance/significance not only to the study of the process of laser nanosurgery itself, but also to be able to improve the technique of laser nanosurgery by assessing the development of the incision and to study the possible inflicted collateral damage. This workstation has the potential to greatly contribute to the study of nanosurgery in biological samples and it is practical enough to be convenient to every biologist. Its potential to be used in studies of nanosurgery and axon regeneration is vast.

Simultaneous imaging of active processes such as laser nanosurgery is of major importance for both the determination of the accuracy of the process as for the study of all the related dynamic effects. Dynamic effects of femtosecond induced laser nanosurgery in cells and tissues were observed in the model organism *C. elegans* and a novel tool is presented for the study of these dynamic effects. This showed a great importance/significance not only to the study of the process of laser nanosurgery itself, but also to be able to improve this technique by assessing the development of the incision.

Acknowledgments

The authors would like to thank Dr. Joe Culotti (Samuel Lunenfeld Research Institute, in Toronto) for providing us with the strain. César Alonso-Ortega for strain maintenance. The funding from the Centre for Innovation and Development of Enterprises (Catalan Government, Spain) through the grant RDITSCON07-1-0006, the Spanish Government grant TEC 2006-12654 and Grupo Ferrer. This work has also been partially funded by Fundació Cellex Barcelona and the Fast Dot program (FP7-ICT-2007-2 (224338)). Authors Susana I. C. O. Santos, Manoj Mathew both contributed equally to this work

#119494 - $15.00 USD Received 3 Nov 2009; revised 18 Dec 2009; accepted 18 Dec 2009; published 24 Dec 2009